Three-Parameter ATP/ATPDraw Transmission Line High Impedance Fault Model

Felipe V. Lopes, Eduardo P. Ribeiro, Raphael L. A. Reis, Kleber M. Silva, Amauri M. Britto, Caio M. Moraes, Rodrigo L. Agostinho, Marco A. M. Rodrigues

***Abstract*—This paper presents a three-parameter transmission line high impedance fault (HIF) model for the Alternative Transients Program (ATP)/ATPDraw. Real-world HIFs caused by vegetation contact on lines belonging to a Brazilian utility are firstly investigated to identify representative features of the fault resistance behavior during the disturbance period. Then, a data regression method is applied to obtain a time-domain function which emulates the fault resistance. Finally, an ATP/ATPDraw transmission line HIF model is developed and described in detail. For the sake of simplicity, only three parameters are proposed to be used in the model, namely: Initial resistance, final resistance and resistance decaying time constant. To prove the proposed model is representative, real HIF records are compared against ATP/ATPDraw simulated ones. The obtained results show the proposed model satisfactorily emulates the effects of real HIFs.**

***Keywords*—ATP/ATPDraw, data regression, fault resistance, high impedance fault, transmission line, power systems.**

I. Introduction

AMONG the various disturbances that can occur on transmission lines, short-circuits (popularly called faults) are undoubtedly in a prominent position [1]. It is well-known that fault current levels are inversely proportional to fault resistances R_f. Hence, depending on the R_f behavior, difficulties in power system monitoring applications, such as protection and fault location schemes, may take place [2], [3].

If R_f is small, high fault currents are expected, and voltages on the fault branch are close to zero. It reduces both protection and fault location performance issues, since the infeed effect does not occur at the fault point [2], [3]. On other hand, if R_f is high, fault currents are reduced, and a certain level of voltage is maintained on the fault branch, through which the sum of local and remote fault current contributions flow. Consequently, in this case, an infeed effect takes place, which can jeopardize the reliability of protection schemes and accuracy of fault location procedures, especially those based on one-terminal data [2], [3]. These scenarios can be much harder to deal with when R_f has a non-linear behavior, which is typically observed in HIF cases [4].

F. V. Lopes and Raphael L. A. Reis are with Federal University of Paraíba (UFPB), Brazil (email: {felipelopes, raphael.leite}@cear.ufpb.br).

Eduardo P. Ribeiro, Kleber M. Silva, Amauri M. Britto, Caio M. Moraes are with University of Brasília (UnB), Brazil (email: {eduardopassos, klebermelo, amaurigm, caiomoraes}@lapse.unb.br).

Rodrigo L. Agostinho is with Evoltz, Brazil (email: rodrigo.lehnemann@evoltz.com.br).

Marco A. M. Rodrigues is with CEPEL, Brazil (email: mamr@cepel.br).

Paper submitted to the International Conference on Power Systems Transients (IPST2023) in Thessaloniki, Greece, June 12-15, 2023.

As a result of the presented context, several works have focused on the development of HIF models for transmission and distribution network studies [4]–[13]. In [4] and [5], ATP/ATPDraw HIF models for distribution networks are reported. In [4], HIF faults are applied in a real distribution system in order to obtain the R_f signature for several soil types. Two time-varying resistances are used, being the first one defined based on the methodology reported in [6], and the second one by means of a polynomial regression technique applied to R_f values obtained from the reported field tests. On the other hand, the model presented in [5] is implemented via ATP/MODELS language functions, which, in conjunction to Transient Analysis of Control System (TACS) elements, reproduce the dynamic of arc resistances. Both models are realistic, but there are implementation details which are not sufficiently explained, posing difficulties on their reproduction. Moreover, the number of settings required in the model reported in [4], and the lack of explanations on how to reproduce real HIF cases in [5] are considered limiting factors.

In [7], HIF models previously presented in [6], [8] and [9] are developed in the EMTP-RV platform. Implementation steps are only briefly described, and guidelines to reproduce the main features of real cases are not clearly addressed. Even the original works [6], [8] and [9] focus only on distribution networks, presenting minor instructions about the methodologies applied to emulate actual HIF scenarios.

In [10], a medium voltage HIF model is implemented using the Matlab/Simulink platform, following developments reported in [11]. Also, in [12] and [13], representative HIF models are reported, resulting in realistic simulations. Nevertheless, details on either computational models or methodologies to reproduce real HIFs are not or only partially explained, posing difficulties on the reproduction of these models in real-world studies.

It is important to emphasize that, despite the great number of works about HIFs that have been published over the years, studies on HIF models and associated applications remain as a topic of great interest for utilities worldwide. For instance, recent contributions which deserve recognition regard to: studies about HIF high frequency signatures [14], proposals of HIF data sets [15], application of HIF models to develop disturbance detection methodologies [16], and methods able to properly obtain HIF arc parameters [17]. Concomitantly, to support these other technological routes, HIF models are still evolving, as reported in [18], especially toward adapting each model to particular studies and systems, simplifying them as much as possible.

From the presented literature review, one can identify several aspects that can be taken as important motivation factors to develop new HIF models. Among them, the following stand out: 1) Most HIF models are developed for distribution networks, such that practical HIF modeling procedures for transmission lines are of interest; 2) Provided details on HIF models are often insufficient to reproduce them. Thereby, providing detailed guidelines for HIF modeling is also very welcome; 3) The most accurate HIF models require several input parameters, which usually results in confusing physical meaning of the model. Thus, simplified models with reduced number of parameters and with clear physical meaning is of great interest; 4) Utilities are usually interested in HIF models capable of approximating simulations to real-world HIF cases; 5) Description of HIF models in free-license simulation platforms, such as the ATP/ATPDraw, is a facilitating factor to spread out them.

Considering the above-mentioned motivating aspects, in this paper, a three-parameter HIF model is proposed for Electromagnetic Transients Programs (EMTP), using the ATP/ATPDraw environment to develop it. Hence, the main contributions of this paper can be listed as being: 1) Innovative studies for transmission HIF modeling are presented; 2) A detailed description of the HIF model for transmission lines is explained, which is expected to allow its ease reproduction in EMTP; 3) A balance between model accuracy, number of input parameters and complexity is taken into consideration, maintaining a clear physical meaning of the used HIF model settings; 4) The proposed HIF modeling methodology allows to obtain an acceptable model approximation of real-world transmission line HIFs on vegetation; and 5) The model is developed using the ATP/ATPDraw environment, which is a free-license platform.

The developments are carried out considering fault features observed in actual records generated from HIFs on vegetation that took place on lines belonging to a Brazilian transmission utility. The presented modeling methodology is divided into three-steps, namely: 1) Main HIF features identification; 2) Estimation of a three-parameter function to represent the fault resistance behavior over the disturbance period; and 3) HIF model development in ATP/ATPDraw, including the description of implementation details required for posterior reproduction. To validate the proposed HIF model, real transmission line HIF scenarios are investigated. The obtained results demonstrate that the proposed three-parameter ATP/ATPDraw model allows realistic emulations of real transmission line HIFs on vegetation, overcoming the need for procedures with excessive complexity.

II. Evaluated Transmission Line HIF Cases

The evaluated HIF scenarios are related to real disturbances that took place on two Brazilian 500 kV/60 Hz double-circuit series compensated lines located in the North region of Brazil, as shown in Fig. 1 (line lengths are presented in the figure). The first line interconnects substations Silves (SIL) and Lechuga (LEC), whereas the other line interconnects substations SIL and Oriximiná (ORX). The rights-of-way of both lines pass through the Amazon Rainforest, where a dense vegetation exists, with several species of trees that can reach relevant heights. As a result, faults on vegetation are frequent in this system, being commonly classified as HIFs.

According to [19] and [20], when a tree branch or stem makes contact with an electrical conductor, there is an arc that starts to burn the tree, causing the vegetation charring phenomenon. Since charred areas along the branch/stem are more conductive, fault currents gradually increase as the charred parts on the tree expand. It occurs until a given stabilization point, when the fault path resistance R_f stops varying, leading currents and voltages to stabilize. Thus, the challenge here is to model the R_f evolving over the fault period, emulating the most representative features of real HIFs.

A. Evaluated Cases

Four real HIF fault scenarios are assessed here. They are studied to identify the main HIF features, specially regarding the R_f evolving during the fault period. Table I lists the studied scenarios, being their respective field voltage and current records (with 256 samples/cycle) illustrated in Fig. 2, where pre-fault, fault and post-fault periods are highlighted.

B. Main Features of the Analyzed HIF Cases

Fig. 2 reveals that the fault period duration can change from case to case, depending on the line protection sensitivity. For instance, Figs. 2(a) and (b) show HIF cases in which the initial R_f value results in currents of about 2000 A. As R_f reduces during the fault period, currents increase approximating to 6000 A six cycles after the fault inception, when the protection is sensitized and the line is opened. On the other hand, in Figs. 2(c) and (d), the initial R_f value results in currents of about 500 A, approximating to 5000 A thirty-five cycles after the

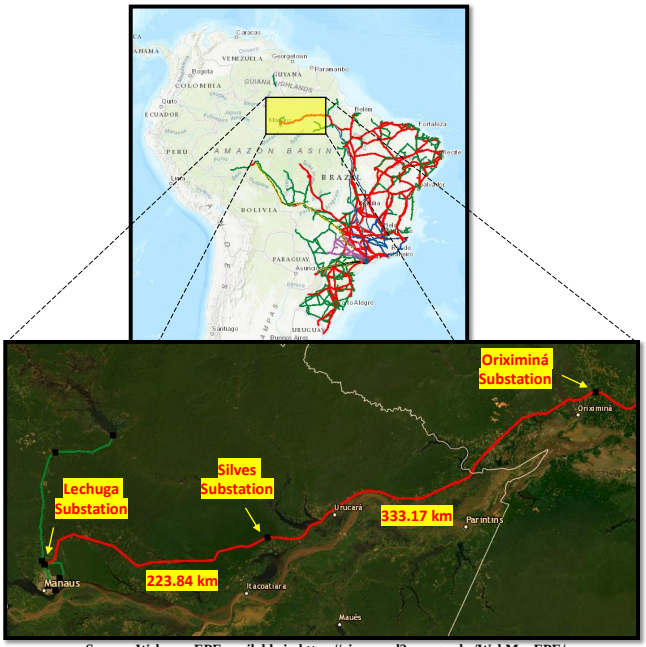

Source: Webmap EPE available in https://gisepeprd2.epe.gov.br/WebMapEPE/

Fig. 1. Location of the studied power transmission network.

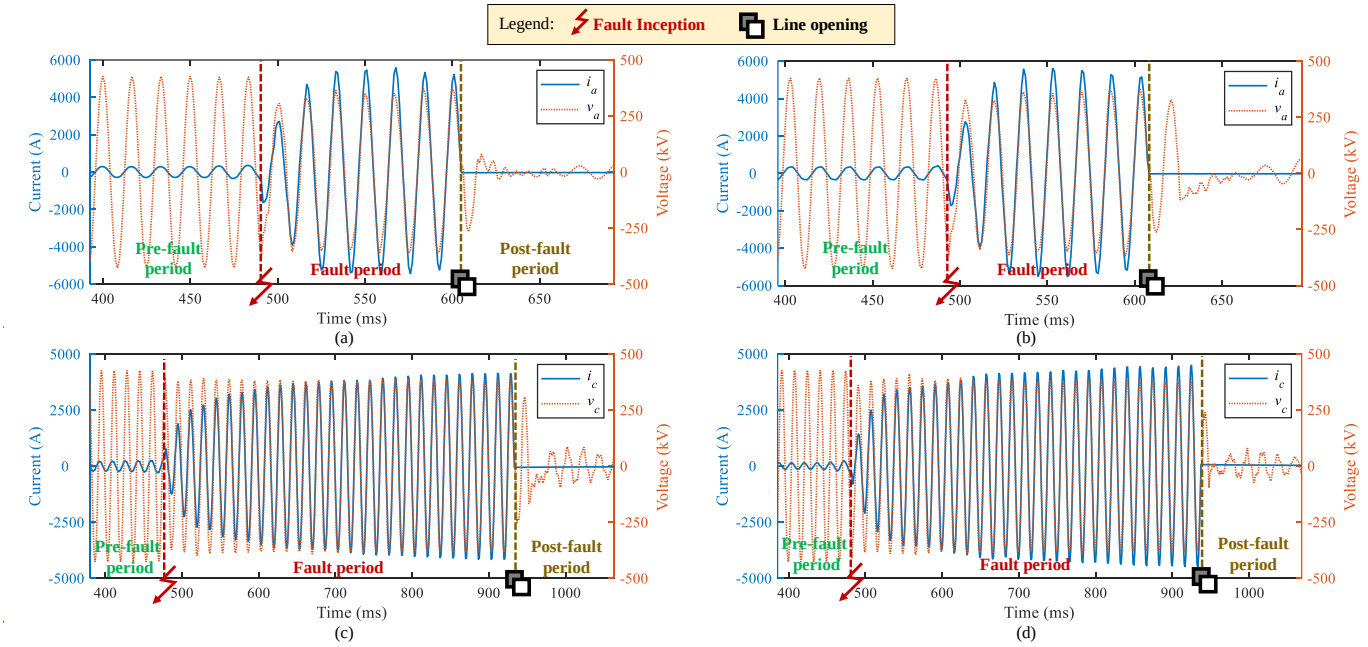

Fig. 2. Evaluated real HIF fault records for cases described in Table I: (a) Case 1; (b) Case 2; (c) Case 3; and (d) Case 4.

fault inception, when the protection issues the line opening command. Thus, from these aspects and analyzing Fig. 2, the following conclusions can be drawn about the analyzed HIFs:

1) Harmonic content presents low amplitude in the fault records. Therefore, it can be disregarded for the sake of simplicity.
2) Voltages and currents are in phase during the fault period, such that the fault path can be approximated by a resistive connection to the ground with a varying R_f.
3) One can identify approximated initial and final R_f values during the fault period. Hereafter, these R_f values will be called $R_{f,ini}$ and $R_{f,end}$, respectively.
4) The transition time constant from $R_{f,ini}$ to $R_{f,end}$ can change from case to case, as shown in Fig. 2. Such R_f decaying time constant will be called τ from now on.
5) Currents increase following a quasi-exponential envelope. It means that the R_f transition from $R_{f,ini}$ to $R_{f,end}$ can be approximated by an exponential decaying with time constant τ. Furthermore, slight current oscillations noticed over the fault period reveal that R_f can slightly oscillate. However, such variations are not considered relevant in the context of this paper, so that they are disregarded for simplification purposes.

A question that can arise on the listed simplifying assumptions regards the suitability of using them to model HIFs in distribution networks rather than on transmission lines, as considered in this paper. It is worth mentioning that the presented assumptions would be representative for HIFs on vegetation without broken conductors in distribution networks. However, if other types of HIFs on distribution feeders are under investigation, such as those with broken conductors that make contact with different surfaces like sand, asphalt, gravel, cobblestones, grass, etc, the representation of intermittence and harmonic content would be relevant, and thus, some of the simplifying assumptions could become invalid.

TABLE I
EVALUATED HIF SCENARIOS.

Case and Faulted Line	Analyzed HIF Scenario
Case 1) Line SIL-LEC, circuit 2	AG fault at 18.72 km from SIL, with $R_f = 250.4\ \Omega$ estimated by the engineering crew. Series compensation was bypassed.
Case 2) Line SIL-LEC, circuit 2	AG fault at 18.00 km from SIL, with $R_f = 258.14\ \Omega$ estimated by the engineering crew. Series compensation was bypassed.
Case 3) Line ORX-SIL, circuit 1	CG fault at 9.66 km from ORX. No information about R_f and series compensation bypass.
Case 4) Line ORX-SIL, circuit 1	CG fault at 6.73 km from ORX. No information about R_f and series compensation bypass.

III. Methodology to Design the Proposed Three-Parameter HIF Model

Based on the considerations highlighted in the previous section, a methodology to design the proposed three-parameter HIF model in ATP/ATPDraw is developed. It is divided into three steps, as illustrated in Fig. 3.

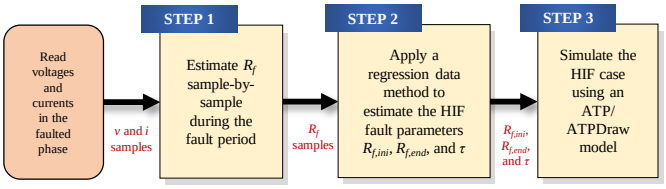

Fig. 3. Methodology to design the proposed three-parameter HIF model.

A. Step 1) Sample-by-Sample Calculation of R_f

The first step consists in calculating R_f sample-by-sample during the fault period. To do so, the fault location method reported in [21] is applied. Such a technique takes R_f as an unknown variable, such that it is estimated in conjunction to the fault distance d from a reference bus (here taken as the line local terminal). Therefore, the following equations are applied:

$$d = \frac{\left(a_1 - \frac{a_3 b_1}{b_3}\right) \pm \sqrt{\left(a_1 - \frac{a_3 b_1}{b_3}\right)^2 - 4\left(a_2 - \frac{a_3 b_2}{b_3}\right)}}{2} \ , \quad (1)$$

$$R_f = \frac{b_2 - d \cdot b_1}{b_3} \ , \quad (2)$$

being:

$$a_1 + jb_1 = \frac{\widehat{V}_L}{Z_{L1}\widehat{I}_L} + \left(1 + \frac{Z_{RS1}}{Z_{L1}}\right), \quad (3)$$

$$a_2 + jb_2 = \left(1 + \frac{Z_{RS1}}{Z_{L1}}\right) \cdot \frac{\widehat{V}_L}{Z_{L1}\widehat{I}_L}, \quad (4)$$

$$a_3 + jb_3 = \frac{\Delta\widehat{I}_L}{Z_{L1}\widehat{I}_L} \cdot \left(1 + \frac{Z_{LS1} + Z_{RS1}}{Z_{L1}}\right), \quad (5)$$

where Z_{LS1} and Z_{RS1} are the positive sequence impedances of line local and remote Thevenin equivalent sources, respectively, $\widehat{V}_L$, $\widehat{I}_L$ and $\Delta\widehat{I}_L$ are the fault loop voltage, current and incremental current phasors measured at the local terminal, respectively, and Z_{L1} is the positive sequence line impedance.

It is worth mentioning that, in (1), two d estimations are calculated, such that the valid one must be selected [21]. Hence, only the d per unit value estimation in between 0 and 1 pu is taken as valid, being the other one discarded. Moreover, an important calculation step regards the Thevenin equivalent impedances Z_{LS1} and Z_{RS1}. Here, $Z_{RS1} = Z_{LS1}$ is assumed to avoid the need for remote data, being Z_{LS1} calculated using:

$$Z_{LS1} = -\frac{\Delta\widehat{V}_L}{\Delta\widehat{I}_L} \ , \quad (6)$$

where $\Delta\widehat{V}_L$ is the local fault loop incremental voltage.

In this paper, phasors are estimated by using the modified cosine filter [22], considering samples directly obtained from the analyzed HIF records. By doing so, R_f is estimated via (2) at each sampling instant during the whole fault period.

Regarding the procedures presented in this section, it is worth noting that neither the fault distance estimation d nor the fault resistance R_f consist in parameters of the proposed HIF model, but rather, they are auxiliary variables which are required to be calculated only when real-world HIF scenarios are desired to be reproduced by means of the proposed model in ATP/ATPDraw simulations. As it will be explained later on, the HIF model parameters can be freely modified by the users, if desired, without requiring the application of (1) and (2) if fictitious HIF cases or already calculated real-world HIF scenarios are of interest.

B. Step 2) Estimation of HIF Characteristic Parameters

The proposed modeling methodology calculates the HIF characteristic parameters via regression procedures. To do so, a reference formula and the respective parameters must be chosen to represent the HIF resistance R_f. Such definitions are of paramount importance for the model performance, because the reference formula and used parameters are those which will dictate the model complexity and accuracy. Indeed, if inappropriate choices are taken, unrepresentative models with unnecessary complexities can be obtained. On the other hand, if reference formulas and parameters are properly chosen, the regression accuracy tends to be improved, especially if the number of unknown parameters increase. Thereby, a balance between model complexity, number of parameters, and model accuracy must exist.

In this paper, a reference formula with three parameters is taken into account, which is considered sufficient to properly represent the main HIF effects, despite eventual slight deviations that can be observed in relation to R_f values obtained from real records. By doing so, excessive complexity in modeling procedures is avoided, maintaining a clear physical meaning of the model parameters. Even so, it is important to mention that, in future works, the authors intend to analyze the benefits of using other possible reference formulas, with different number of parameters.

Once R_f samples are obtained from (2), the three parameters of interest can be estimated, namely: 1) Initial fault resistance $R_{f,ini}$; 2) Final fault resistance $R_{f,end}$; 3) R_f decaying time constant τ. As $R_{f,ini}$ is assumed here to exponentially reduce until $R_{f,end}$ with a decaying time constant τ, the $R_f(t)$ function defined over the time t can be expressed by:

$$R_f(t) = R_{f,end} + (R_{f,ini} - R_{f,end}) \cdot e^{[-\tau \cdot (t - t_0)]} \ , \quad (7)$$

where t_0 is the fault inception instant, which is compensated to be $t_0 = 0$ s in the analyzed cases. Thus, aiming to apply an exponential data regression, (7) is rewritten as:

$$R_f(t) = \alpha + \beta \cdot e^{(-\tau \cdot t)} \ , \quad (8)$$

being $\alpha = R_{f,end}$ and $\beta = R_{f,ini} - R_{f,end}$.

Since α, β and τ are estimated from the regression procedure, $R_{f,end}$ and τ can be directly obtained. On the other hand, $R_{f,ini}$ must be calculated using $R_{f,ini} = \beta + R_{f,end}$. Then, these three parameters ($R_{f,ini}$, $R_{f,end}$ and τ) are set in a practical ATP/ATPDraw HIF model, allowing realistic HIF simulations. Table II summarizes the regression results in terms of the estimated α, β and τ coefficients and their respective 95% confidence bounds obtained for the real HIF cases shown previously in Fig. 2. The used Matlab code applied to perform the regression procedure is presented in Fig. 4. Moreover, the reference R_f behaviors and the estimated ones for the analyzed real HIF records are compared in Fig. 5, where the estimated $R_{f,ini}$, $R_{f,end}$ and τ values are highlighted.

Analyzing the obtained results, it is noticed that the estimated R_f functions are adherent to the reference R_f behavior. It is important to explain that, although there are

TABLE II
RESULTS OBTAINED FROM THE REGRESSION PROCEDURE

Evaluated Case	Coefficients (with 95% confidence bounds)
Case 1	$\alpha = 57.73\ (55.35, 60.12)$, $\beta = 229.50\ (212.30, 246.60)$ $\tau = 247.40\ (216.30, 278.60)$
Case 2	$\alpha = 57.76\ (55.61, 59.92)$ $\beta = 193.00\ (178.60, 207.30)$ $\tau = 202.70\ (177.60, 227.70)$
Case 3	$\alpha = 97.22\ (94.71, 99.73)$ $\beta = 494.50\ (467.70, 521.30)$ $\tau = 89.03\ (81.70, 96.37)$
Case 4	$\alpha = 84.7\ (82.9, 86.51)$ $\beta = 313.3\ (295.8, 330.8)$ $\tau = 73.7\ (67.42, 79.98$

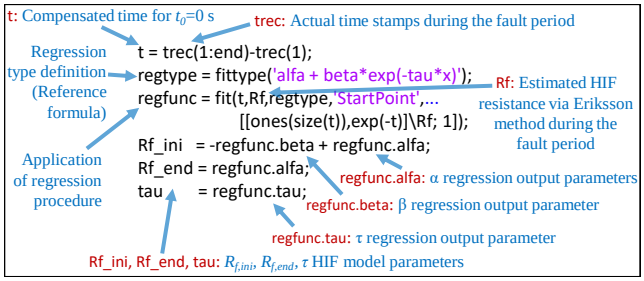

Fig. 4. Alternative Matlab code to apply the R_f regression procedure.

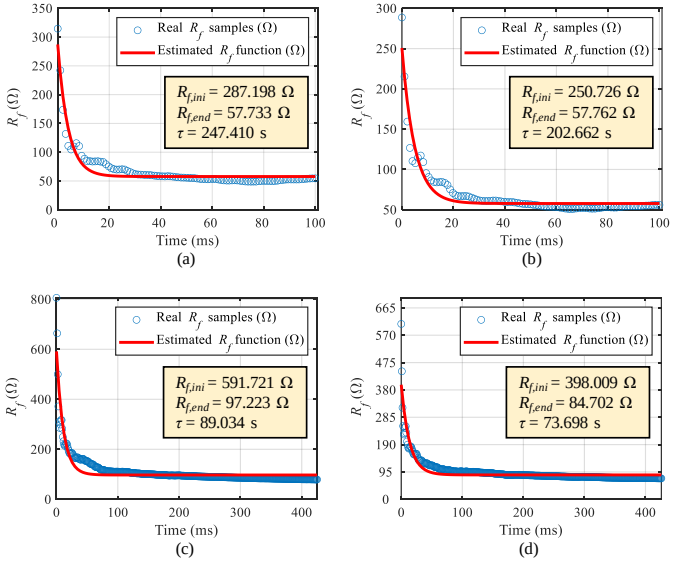

Fig. 5. Obtained regression results for the analyzed real HIF scenarios: (a) Case 1; (b) Case 2; (c) Case 3; and (d) Case 4.

some regions on the graphics (in Fig. 5) where discrepancies are verified, they are not significant from the perspective of properly representing the main features of HIFs. For instance, there are slight oscillations in the real R_f samples in the first moments of the fault period which are not represented in the estimated R_f functions. As mentioned earlier, these little differences are caused by the simplifications considered when deciding about the reference regression formula. Thereby, in the context of this work, these discrepancies are not considered critical for practical studies in detriment of the facilities achieved by incorporating such simplifications.

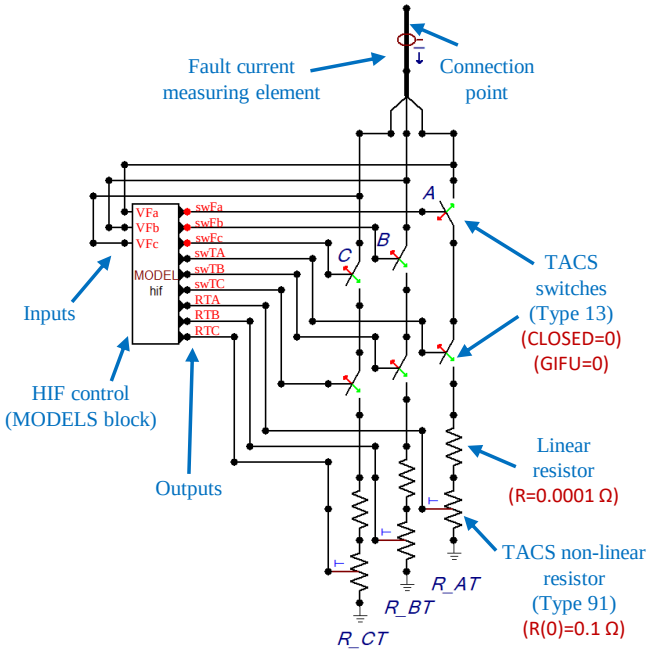

Fig. 6. Proposed HIF model.

It is also important to recognize that deviations in the estimated $R_{f,ini}$, $R_{f,end}$ and τ parameters are expected to occur, since the estimation of R_f reference values are prone to errors as well. Even so, the main features of the HIF are properly represented, thus making the proposed model promising for HIF studies on transmission lines. Indeed, the simplified data regression makes the calculation of the HIF parameters easier, maintaining a clear physical meaning of the model settings. Therefore, the authors consider that there is a satisfactory balance between accuracy and simplicity, allowing realistic simulations of HIF scenarios on transmission lines.

A practical finding obtained from the analyzed HIF scenarios regards the range of settings that could be used in $R_{f,ini}$, $R_{f,end}$ and τ to realistically represent HIF cases. Fig. 5 demonstrates that these parameters can significantly vary for different scenarios. Even so, one can conclude that $R_{f,ini}$ and $R_{f,end}$ are of the order of hundreds and dozens of ohms, respectively, whereas τ varies from dozens to hundreds of seconds, depending on the vegetation charring speed. From the analyzed records, it is noticed that, if the transition period from $R_{f,ini}$ to $R_{f,end}$ is of about 10-30 power cycles, τ of the order of 70-90 seconds can be used. On the other hand, if such a transition occurs within a period of about 4-7 power cycles, τ must be increased to 200-250 seconds. However, previous experiences in evaluating HIFs on vegetation reveal that τ can be even higher, reaching the order of 400-500 seconds.

C. Step 3) ATP/ATPDraw HIF Modeling

The last step consists in implementing a HIF model in ATP/ATPDraw platform. To do so, native ATP/ATPDraw tools are used, including TACs elements and MODELS programming blocks. Fig. 6 illustrates the proposed model, pointing out the default settings of the used elements, as well as the names of inputs and outputs.

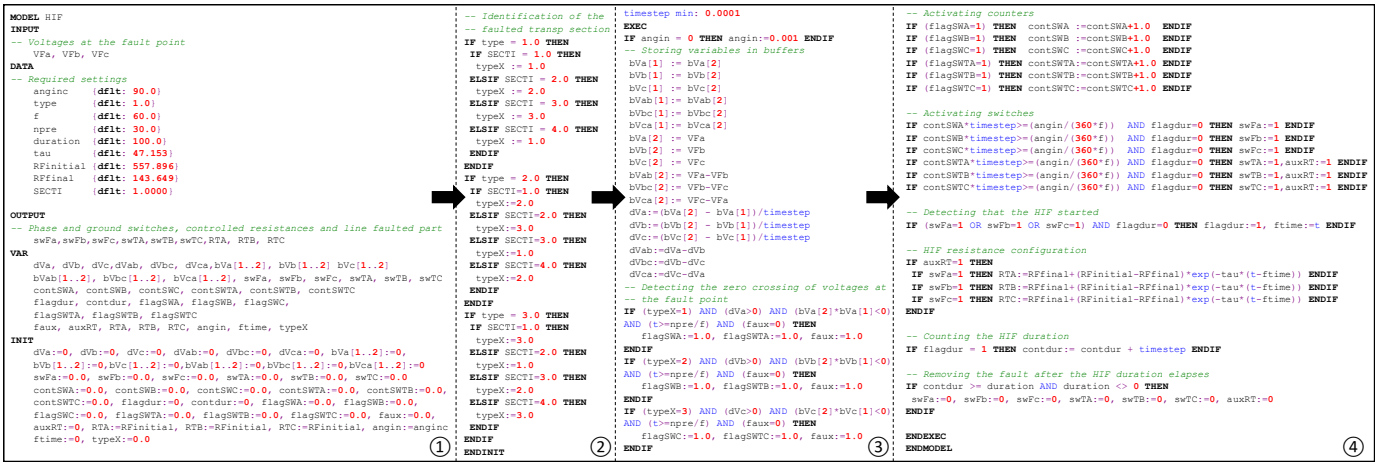

Fig. 7. MODELS code to control the HIF elements, where arrows indicate the code sequential flow.

The main elements in the proposed HIF model are: TACS switches, which dictate the fault inception instants, determining the fault type; TACS resistances, which are controlled to represent the R_f function obtained via data regression; and HIF control block programmed using the MODELS language, whose associated code is presented in Fig. 7. Other elements like current measuring sensors and linear resistors are applied for secondary purposes, such as to separate electrical nodes and to provide auxiliary measurements that can be useful in practical studies. The settings of these auxiliary elements are indicated in the figure.

Variables $R_{f,ini}$, $R_{f,end}$ and τ are inputs of the HIF model, being represented by `RFinitial`, `RFfinal` and `tau`, respectively (see Fig. 7). Since HIFs are typically single-phase-to-ground faults, the model is programmed to simulate only AG, BG and CG faults. To do so, the input parameter `type` (1=AG, 2=BG and 3=CG) is included. Moreover, in order to properly represent these fault types when the line transposition is modeled in ATP/ATPDraw, the variable `SECTI` is created. It adapts the HIF type according to an $\frac{1}{6} - \frac{1}{3} - \frac{1}{3} - \frac{1}{6}$ transposition scheme, so that `SECTI` equal to 1, 2, 3 or 4 must be set to represent HIFs on the first, second, third or fourth transposition section. Other transposition schemes are not considered.

In addition to the mentioned auxiliary input parameters, the number of pre-fault cycles, fault inception angle θ and fault duration are also considered, being represented by the settings `npre`, `anginc` and `duration`, respectively (see Fig. 7). `npre` defines the number of cycles before the fault application switch is activated. As soon as a period equivalent to `npre` fundamental cycles elapses, the point on wave that represents θ is detected (assuming a sinusoidal reference), according to the setting `anginc`. Derivatives and zero crossings of voltages at the fault point are analyzed to automatically detect θ, and as soon as it occurs, the fault is connected to the system. Then, a counter remains activated during a time period equal to the setting `duration`. After that, the fault switch is opened, disconnecting it from the circuit. Hence, to maintain the fault connected, `duration` must be set with values higher than the total simulation time.

It is important to explain that the three inputs at the left side of the HIF control block (see Fig. 6) consist in voltage inputs. They receive information about voltages at the fault point, which are represented in the MODELS code by `VFa`, `VFb` and `VFc` (see Figs. 6 and 7). On the other hand, on the right side of the HIF control block, one can see several outputs. Basically, outputs `swFa`, `swFb` and `swFc` control phase switches, outputs `swTA`, `swTB` and `swTC` control ground switches, and outputs `RTA`, `RTB` and `RTC` control the HIF fault resistance values, emulating the R_f estimated function, described by (7). All the remaining calculation procedures can be found in the MODELS code provided in Fig. 7. In this paper, the ATPDraw 7.2 version was used in conjunction to the ATP Launcher version 1.19.

IV. Evaluation of the Proposed HIF Modeling and Simulation Methodology

In this section, the proposed three-parameter HIF model is evaluated in two steps: 1) Verification of the proposed model capability to properly emulate the main HIF features; 2) Model validation by comparing real and simulated HIF records.

Aiming at the above-mentioned studies, a detailed model of the power system illustrated in Fig. 1 is used to simulate HIF scenarios. Therefore, the case studies could be approximated as much as possible to the real cases described in Table I, including the application of protection elements which open the lines at instants compatible to those observed in the real records. By doing so, pre-fault, fault and post-fault periods could be verified in the simulated waveforms.

Among the analyzed scenarios, from Fig. 2, it is noticed that cases 1 and 2, as well as cases 3 and 4 are very similar to each other. Hence, due to space limitations, only cases 1 and 3 are chosen to be analyzed. Still in this context, it is worth mentioning that the used ATP/ATPDraw power system model was provided by the owner of the analyzed 500 kV/60 Hz lines SIL-LEC and ORX-SIL, consisting in the same model used during the system pre-operational studies, i.e., it is a validated and realistic model.

A. Verification of Proposed Model Capability to Represent the Main HIF Features

In this first evaluation step, HIF simulations in the studied power system ATP/ATPDraw model are carried out with the intention to verify whether the proposed three-parameter HIF model is capable of properly simulating the main HIF features over the fault period. Fig. 8 presents the simulated voltage and current records for cases 1 and 3, considering the HIF parameters set in accordance to the $R_{f,ini}$, $R_{f,end}$ and τ values shown in Fig. 5.

In both scenarios, current and voltage waveforms met the expected behaviors according the assumptions presented in Section II-B. Indeed, voltage and currents are in phase, and currents increase following an exponential envelope, which is very close to the quasi-exponential one observed in the analyzed real-world HIF cases. Therefore, it is proven that the model allows to vary the time decaying constant τ to simulate slower or faster transitions between $R_{f,ini}$ and $R_{f,end}$, which can be also adjusted to vary the initial and final R_f values in the event of interest. Undoubtedly, since these parameters have a clear physical meaning, the proposed model becomes easier to set than other existing approaches.

B. Proposed Model Validation

The proposed three-parameter HIF model is validated by comparing real and simulated HIF records related to cases 1 and 3 described in Table I. Despite the efforts to adjust the simulated ATP/ATPDraw power system model at the same operation condition found in the real records, slight differences in the system loading profile were found. Indeed, the ATP/ATPDraw power system model has elements which are difficult to set exactly as in the real HIF scenarios. Thus, to provide a better comparison between the overall behavior of signals in the real and simulated records, an approximated HIF simulation is considered, being currents and voltages analyzed in per unit values. The results obtained for cases 1 and 3 are presented in Figs. 9 and 10, respectively.

Analyzing the results, it is noticed that the proposed model has fitted very well to the analyzed real-world cases. It proves the proposed model validity, and demonstrates that it is reliable for HIF simulations on transmission lines. Even so, the found discrepancies are discussed next.

Comparing Figs. 9 and 10, it is noticed that the HIF model was very accurate in the first 100 ms of the fault period. However, in case 3, as the fault remains on the system, slight discrepancies are verified in current and voltage levels at the final moments of the disturbance. It can be explained by the use of a simplified three-parameter regression formula, which leads to errors, mainly in $R_{f,end}$ and τ. Such deviations could be compensated by considering more complex regression strategies, but here, the focus is to maintain a satisfactory balance between accuracy and simplicity, maintaining a clear

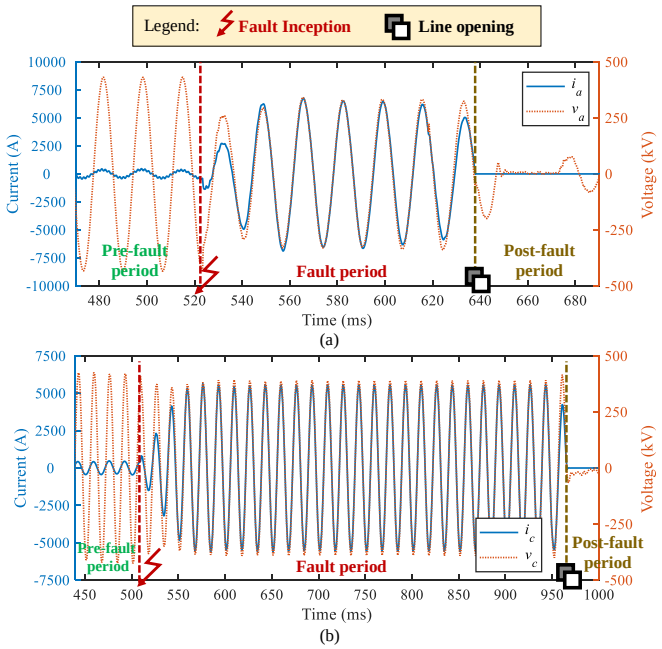

Fig. 8. Analysis of the main HIF features simulated in ATP/ATPDraw via proposed model: (a) Case 1; (b) Case 3.

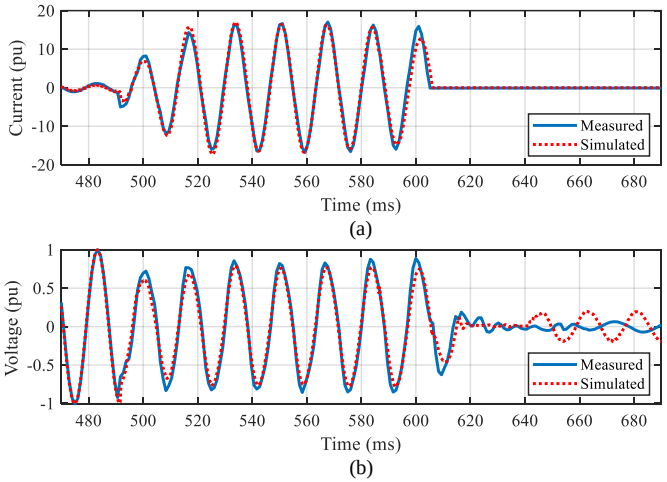

Fig. 9. Comparison between measured and simulated quantities in the faulted phase for case 1: (a) Current record in pu; (b) Voltage record in pu.

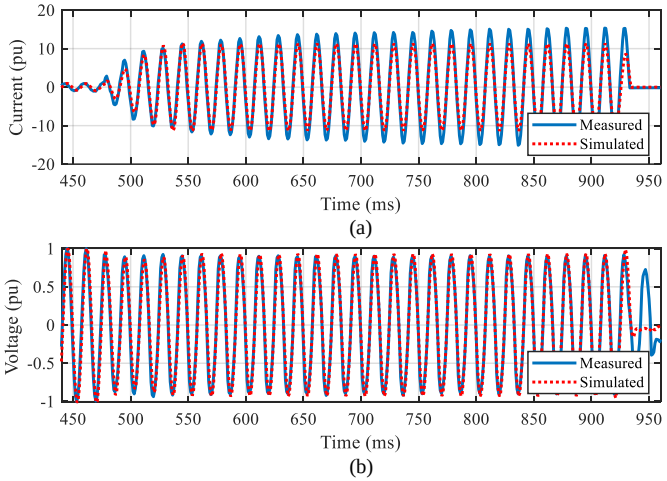

Fig. 10. Comparison between measured and simulated quantities in the faulted phase for case 3: (a) Current record in pu; (b) Voltage record in pu.

physical meaning of the HIF model. Thus, considering that there is some unpredictable aspects on the way the vegetation charring phenomenon occurs, $R_{f,ini}$, $R_{f,end}$ and τ can significantly vary from case to case. Hence, in the authors' opinion, the proposed HIF is indeed representative, irrespective of the found discrepancies, being useful for HIF studies on transmission lines, specially because it guarantees the representation of the main HIF features by using settings with clear physical meaning. Even so, to minimize eventual discrepancies between simulated and real records in the initial and final stages of the fault period, $R_{f,ini}$, $R_{f,end}$ and τ can be changed, as desired by the model users.

V. Conclusions

In this paper, a three-parameter transmission line HIF model is proposed. The design methodology and its associated modeling procedures in the ATP/ATPDraw environment are described in detail. To do so, four real HIF scenarios that took place on 500 kV/60 Hz transmission lines in operation in Brazil are taken into account, allowing to analyze the main HIF features to be reproduced in the proposed model.

In the first part of the design methodology, the real HIF records are analyzed to study and estimate the HIF resistance behavior over the fault period. Then, the obtained results are used in a data regression procedure, through which a mathematical function that can emulate the HIF resistance over the time is obtained. Finally, an ATP/ATPDraw model capable of simulating the obtained HIF resistance function is developed by using native tools of such a platform. Used elements, parameters and programming codes are fully described, allowing its reproduction by other interested parties.

Aiming to guarantee a satisfactory balance between accuracy and simplicity, only three parameters are used in the regression model, resulting in three main HIF model settings, namely: initial fault resistance, final fault resistance, and resistance decaying time constant. These parameters are estimated for the four analyzed real HIF cases, being also reported in this paper. The application of the obtained HIF parameters in the developed ATP/ATPDraw model is analyzed, and the model is set to reproduce real HIF records. Such studies revealed the ease to configure the proposed model, since it requires only few parameters to be set, allowing the users to freely modify the parameters, if necessary. Moreover, from the validation case studies, it is demonstrated that the proposed model is reliable and accurate, highlighting its usefulness for studies about transmission line HIFs on vegetation. In future works, it is intended to evaluate the cost-benefit of applying other reference formulas in the regression procedures, considering more than three parameters to represent the HIF resistance behavior over the time.

Acknowledgement

This work was developed in partnership with IATI and CEPEL within the scope of the R&D project PD-06908-0003/2021, sponsored by the Brazilian Agency of Electrical Energy (ANEEL) and EVOLTZ. The authors thank the cooperation of Ms. Larissa Silva (EVOLTZ).

References

[1] W. Stevenson Jr and J. Grainger, *Power system analysis*. McGraw-Hill Education, 1994.

[2] J. L. Blackburn and T. J. Domin, *Protective relaying: principles and applications*. CRC press, 2006.

[3] M. M. Saha, J. J. Izykowski, and E. Rosolowski, *Fault Location on Power Networks*, 1st ed. Springer Publishing Company, Inc., 2009.

[4] W. C. Santos, B. Souza, N. S. Brito, F. B. Costa, and M. Paes, "High impedance faults: From field tests to modeling," *Journal of Control, Autom. and Electrical Systems*, vol. 24, no. 6, pp. 885–896, 2013.

[5] K. M. Shebl, E. A. Badran, and E. Abdalla, "A combined models-tacs atpdraw general model of the high impedance faults in distribution networks," *MEPCON*, vol. 10, pp. 19–21, 2010.

[6] S. Nam, J. Park, Y. Kang, and T. Kim, "A modeling method of a high impedance fault in a distribution system using two series time-varying resistances in emtp," in *2001 Power Engineering Society Summer Meeting. Conference Proceedings*, vol. 2. IEEE, 2001, pp. 1175–1180.

[7] V. C. Nikolaidis, A. D. Patsidis, and A. M. Tsimtsios, "High impedance fault modelling and application of detection techniques with emtp-rv," *The Journal of Engineering*, vol. 2018, no. 15, pp. 1120–1124, 2018.

[8] Y. Sheng and S. M. Rovnyak, "Decision tree-based methodology for high impedance fault detection," *IEEE Transactions on Power Delivery*, vol. 19, no. 2, pp. 533–536, 2004.

[9] N. I. Elkalashy, M. Lehtonen, H. A. Darwish, M. A. Izzularab, and A.-m. I. Taalab, "Modeling and experimental verification of high impedance arcing fault in medium voltage networks," *IEEE Trans. on Dielectrics and Electrical Insulation*, vol. 14, no. 2, pp. 375–383, 2007.

[10] S. Salona, "High impedance fault modelling on 11 kv feeder using matlab simulink," 2016.

[11] A. Emanuel, D. Cyganski, J. Orr, S. Shiller, and E. Gulachenski, "High impedance fault arcing on sandy soil in 15 kv distribution feeders: contributions to the evaluation of the low frequency spectrum," *IEEE Transactions on Power Delivery*, vol. 5, no. 2, pp. 676–686, 1990.

[12] J. Doria-García, C. Orozco-Henao, R. Leborgne, O. D. Montoya, and W. Gil-González, "High impedance fault modeling and location for transmission line," *Electric Power Systems Research*, vol. 196, p. 107202, 2021.

[13] S. Maximov, V. Torres, H. Ruiz, and J. Guardado, "Analytical model for high impedance fault analysis in transmission lines," *Mathematical Problems in Engineering*, vol. 2014, 2014.

[14] D. P. S. Gomes, C. Ozansoy, and A. Ulhaq, "Vegetation high-impedance faults' high-frequency signatures via sparse coding," *IEEE Transactions on Instrumentation and Measurement*, vol. 69, no. 7, pp. 5233–5242, 2020.

[15] D. P. S. Gomes and C. Ozansoy, "Vehif: An accessible vegetation high-impedance fault data set format," *IEEE Transactions on Power Delivery*, vol. 37, no. 6, pp. 5473–5475, 2022.

[16] B. Wang and X. Cui, "Nonlinear modeling analysis and arc high-impedance faults detection in active distribution networks with neutral grounding via petersen coil," *IEEE Transactions on Smart Grid*, vol. 13, no. 3, pp. 1888–1898, 2022.

[17] M. Wei, F. Shi, H. Zhang, F. Yang, and W. Chen, "A high-efficiency method to determine parameters of high impedance arc fault models," *IEEE Transactions on Power Delivery*, vol. 37, no. 2, pp. 1203–1214, 2022.

[18] N. Zamanan and J. Sykulski, "The evolution of high impedance fault modeling," in *16th International Conference on Harmonics and Quality of Power (ICHQP)*, 2014, pp. 77–81.

[19] A. Ajayi, F. S. Osayi, D. K. Jerome, and A. Omoregie, "Investigating vegetation induced faults on power transmission line: A case study of the irrua-auchi-agenebode 33 kv transmission line edo state nigeria," *Global Journal of Advanced Research*, vol. 3, no. 3, pp. 177–183, 2016.

[20] C. Yang, T. Chen, B. Yang, X. Zhang, and S. Fan, "Experimental study of tree ground fault discharge characteristics of 35 kv transmission lines," in *IEEE Sustainable Power and Energy Conference*, 2021, pp. 2883–2891.

[21] L. Eriksson, M. M. Saha, and G. D. Rockefeller, "An accurate fault locator with compensation for apparent reactance in the fault resistance resulting from remore-end infeed," *IEEE Transactions on Power Apparatus and Systems*, vol. PAS-104, no. 2, pp. 423–436, 1985.

[22] D. G. Hart, D. Novosel, and R. A. Smith, *Modified Cosine Filters*, U. S. Patent 6154687 ed., November, 2000.